Inhibition of Src Kinase Blocks High Glucose–Induced EGFR Transactivation and Collagen Synthesis in Mesangial Cells and Prevents Diabetic Nephropathy in Mice

Kanta Taniguchi,[1,2,3] Ling Xia,[1,2,3] Howard J. Goldberg,[1,2,3] Ken W.K. Lee,[1,2,3,4] Anu Shah,[1,2,3,4] Laura Stavar,[1,2,3,4] Elodie A.Y. Masson,[1,2,3] Abdul Momen,[1,5] Eric A. Shikatani,[1,5,6] Rohan John,[1,7] Mansoor Husain,[1,5] and I. George Fantus[1,2,3,4,5]

Chronic exposure to high glucose leads to diabetic nephropathy characterized by increased mesangial matrix protein (e.g., collagen) accumulation. Altered cell signaling and gene expression accompanied by oxidative stress have been documented. The contribution of the tyrosine kinase, c-Src (Src), which is sensitive to oxidative stress, was examined. Cultured rat mesangial cells were exposed to high glucose (25 mmol/L) in the presence and absence of Src inhibitors (PP2, SU6656), Src small interfering RNA (siRNA), and the tumor necrosis factor-α–converting enzyme (TACE) inhibitor, TAPI-2. Src was investigated in vivo by administration of PP2 to streptozotocin (STZ)-induced diabetic DBA2/J mice. High glucose stimulated Src, TACE, epidermal growth factor receptor (EGFR), mitogen-activated protein kinases (MAPKs), extracellular signal–regulated kinase (ERK1/2, p38), and collagen IV accumulation in mesangial cells. PP2 and SU6656 blocked high glucose–stimulated phosphorylation of Src Tyr-416, EGFR, and MAPKs. These inhibitors and Src knockdown by siRNA, as well as TAPI-2, also abrogated high glucose–induced phosphorylation of these targets and collagen IV accumulation. In STZ-diabetic mice, albuminuria, increased Src pTyr-416, TACE activation, ERK and EGFR phosphorylation, glomerular collagen accumulation, and podocyte loss were inhibited by PP2. These data indicate a role for Src in a high glucose-Src-TACE-heparin-binding epidermal growth factor-EGFR-MAPK–signaling pathway to collagen accumulation. Thus, Src may provide a novel therapeutic target for diabetic nephropathy. ***Diabetes*** **62:3874–3886, 2013**

Diabetic nephropathy, the leading cause of end-stage renal disease in the Western world, is a consequence of sustained hyperglycemia (1–3). Mesangial extracellular matrix (ECM) accumulation reflects increased protein synthesis such as collagen IV, fibronectin, and laminin (1–6). Decreased ECM degradation also occurs due to increased plasminogen activator inhibitor (PAI-1) expression (7). Excessive ECM elaboration has been determined to involve activation of multiple signaling abnormalities such as angiotensin and transforming growth factor-β (TGF-β) (1–4,8). Pertinent intracellular biochemical derangements that have been implicated include increases in advanced glycation end products (AGEs), polyol and hexosamine pathway flux, reactive oxygen species (ROS), and the activities of protein kinase C (PKC), extracellular signal–regulated kinase (ERK), p38, Akt, Jak, and rho kinase (1–4,8–10).

c-Src (Src), a 60-kDa proto-oncogene, is the prototype of a family of membrane-associated nonreceptor tyrosine kinases, the Src family kinases (SFKs) (11,12). Src has a low basal activity due to intramolecular interactions but is activated by receptor tyrosine kinases, such as the epidermal growth factor receptor (EGFR), and by a variety of other stimuli that are altered in the diabetic milieu, including G-protein coupled receptors (GCPRs), TGF-β, and ROS (11–15). Further, relevant to diabetic nephropathy, Src activates Akt and ERK and increases ROS generation (11,12,16). One study reported Src was activated by high glucose in mesangial cells (17) and, recently, in the glomeruli of rats with streptozotocin (STZ)-induced diabetes (18). Furthermore, Src was found to be required for angiotensin or TGF-β–induced collagen expression in mesangial cells (13,15,18). However, the contribution of Src to the effects of high ambient glucose (high glucose) on collagen IV synthesis in mesangial cells and its general importance in the pathogenesis of diabetic nephropathy are unclear.

Receptor tyrosine kinases, including EGFR, undergo dimerization and autophosphorylation after ligand-binding (19). Intriguingly, a complex relationship exists between Src and EGFR. EGFR activates Src and is phosphorylated by Src on Tyr-845, which has been associated with Stat 5b recruitment and mitogenesis (12,19,20). Furthermore, Src may also function upstream of EGFR and is required for EGFR transactivation by GPCRs, cytokines, and other stimuli in what is referred to as the triple membrane-spanning (TMS) pathway (15,20–23). In this signaling cascade, membrane-bound EGFR proligands, such as heparin-binding epidermal growth factor (HB-EGF), are cleaved by proteases and bind to EGFR, enabling them to activate downstream kinases such as ERK and Akt (20,21–26). Depending on the ligand and cell type, different cell surface enzymes containing a disintegrin and metalloprotease domain (ADAMs) have been implicated as sheddases for EGFR ligands, including tumor necrosis factor-α–converting enzyme (ADAM17/TACE) (23–27).

In this study, we found that Src activation by high glucose mediated EGFR transactivation, leading to mitogen-activated

From the [1]Toronto General Research Institute, University Health Network, University of Toronto, Toronto, Ontario, Canada; the [2]Banting and Best Diabetes Centre, University of Toronto, Toronto, Ontario, Canada; the [3]Department of Medicine and Lunedfeld-Tanenbaum Research Institute, Mount Sinai Hospital, Toronto, Ontario, Canada; the [4]Department of Physiology, University of Toronto, Toronto, Ontario, Canada; the [5]Heart and Stroke Richard Lewar Center for Excellence in Cardiovascular Research, University of Toronto, Toronto, Ontario, Canada; the [6]Department of Laboratory Medicine and Pathobiology, University of Toronto, Toronto, Ontario, Canada; and the [7]Department of Pathology, University Health Network, University of Toronto, Toronto, Ontario, Canada.

Corresponding author: I. George Fantus, gfantus@mtsinai.on.ca.

Received 26 July 2012 and accepted 27 July 2013.

DOI: 10.2337/db12-1010

This article contains Supplementary Data online at http://diabetes.diabetesjournals.org/lookup/suppl/doi:10.2337/db12-1010/-/DC1.

K.T. and L.X. contributed equally to this work.

protein kinase (MAPK) activation and collagen IV synthesis. These observations in cultured mesangial cells were extended to a mouse model of type 1 diabetes in which Src inhibition prevented several characteristic features of diabetic nephropathy, indicating that this signaling pathway serves as a key pathophysiological mechanism.

RESEARCH DESIGN AND METHODS

Cell culture. Primary rat glomerular mesangial cells (passages 8–12) were isolated, characterized, and grown as described (9). At 70–80% confluence, cells were growth-arrested in Dulbecco's modified Eagle's medium (DMEM) containing 0.1% FBS, and 5.6 mmol/L (normal glucose) or 25 mmol/L (high glucose) D-glucose or normal glucose plus 19.4 mmol/L mannitol as an osmotic control. For inhibitor studies, cells were treated as follows: PP2 (2 μmol/L) and SU6656 (2.5 μmol/L), TAPI-2 (100 μmol/L) (Calbiochem, San Diego, CA). For experiments with 48-h exposure to high glucose, PP2 and SU6656 were added for the final 24 h. For time course studies of 24 h or less, these inhibitors were added 1 h before high glucose. TAPI-2 and AG1478 were added 1 h before high glucose in all experiments. AG1478 (200 nmol/L) (Biomol, Plymouth Meeting, PA) was added 30 min before EGF. All inhibitors were dissolved in DMSO. Control cells received an equal amount of DMSO.

Small interfering RNA transfection. A stealth negative universal control scrambled (Src), two different Src-specific Stealth RNAi duplex oligoribonucleotides (Src-RSS331230-1), and a Fyn-specific Stealth RNAi duplex oligoribonucleotide (Fyn-RSS303099) were predesigned (Invitrogen). Reverse transfections were performed according to the manufacturer's protocol. Briefly, small interfering RNA (siRNA) (5 nmol/L) was mixed with lipofectamine RNAiMax in serum-free Opti-MEM and incubated for 20 min at room temperature. Then, 200 μL was added into each well containing mesangial cells (2×10^5) in 1.8 mL DMEM (10% FBS without antibiotics). After 24 h, cells were growth-arrested in 5.6 mmol/L or 25 mmol/L glucose for 48 h.

Immunoprecipitation. Total cell lysates (500 μg) were incubated with 3 μg anti-Src monoclonal antibodies (Cell Signaling), anti-Fyn (Novus Biologicals), or anti-Yes (BD Biosciences) and protein-A Sepharose (GE Healthcare) for 1 h at 4°C. Immune complexes were washed and eluted with cell lysis buffer (120 μL). Gel loading buffer (40 μL of 4× Laemmli buffer) was added, and samples were boiled at 100°C for 5 min. Equal amounts were separated by SDS-PAGE and immunoblotted.

Immunoblotting. Kidney cortex, mesangial cell total lysates, and membrane fractions were prepared and underwent immunoblotting, as previously described (9). Primary antibodies against SrcpTyr-416, EGFRpTyr-845, EGFRpTyr-1173, phospho-ERK, phospho-p38, and total EGFR, Src, ERK, p38, TACE, Fyn, Yes (Cell Signaling), and collagen IV (Cederlane, Burlington, Ontario, Canada) were used at 1:1,000 dilution. p-ERK (1:3,000) goat anti–HB-EGF (Sc-21591) (1:1,000), β-actin, and horseradish peroxidase–conjugated secondary antibodies were from Santa Cruz Biotechnology, Inc.

Confocal immunofluorescence microscopy. Collagen IV and TACE were detected as described (9) by growing mesangial cells on coverslips in six-well plates and staining with primary collagen IV (1:300, Rockland Immunochemicals) or TACE (1:200, Abcam) antibodies, followed by fluorescein isothiocyanate–conjugated goat anti-rabbit IgG (Jackson ImmunoResearch). FM 4-64FX dye, a lipophilic styryl compound (Invitrogen), was used for labeling the plasma membrane of the cells according to the manufacturer's instructions. Immunofluorescence was detected by confocal microscopy, and the fluorescence intensities of plasma membranes and total cells were analyzed by Scion Image Software (Scion Corporation).

TACE activity assay. Mesangial cell lysates and kidney cortex homogenates were analyzed for TACE activity using SensoLyte520 TACE Activity Assay Kit (AnaSpec Inc.), following the manufacturer's instructions. Enzymatic activity was measured using a fluorescence resonance energy transfer peptide containing the fluorescent probe 5-FAM quenched by QXL520. TACE cleaves the peptide and releases 5-FAM, leading to increased fluorescence.

Animals. Eight-week-old male DBA2/J mice (20–25 g) (The Jackson Laboratory) received five consecutive daily intraperitoneal injections of STZ (Sigma) (40 mg/kg, freshly prepared in 100 mmol/L citrate buffer, pH 4.5) after a 6-h fast (28). Control mice were injected with buffer alone. Six-hour fasting glucose was monitored after 3 weeks via tail vein using a glucometer (OneTouch Ultra, LifeScan) and was more than 15 mmol/L in all of the mice with diabetes. The mice were divided into four groups: control (n = 22), diabetes (n = 25), control + PP2 (n = 23), or diabetes + PP2 (n = 25). The PP2 groups received 2 mg/kg PP2 dissolved in DMSO three times per week by intraperitoneal injection. At 16 weeks of age, individual mice were placed in metabolic cages to obtain urine collections. Urinary albumin excretion was assessed by the urinary albumin-to-creatinine ratio using the Albuwell M kit and The Creatinine Companion (Exocell, Philadelphia, PA). Mice were killed at 18 to 24 weeks after STZ injection. Animal protocols were approved by the University Health Network Animal Care Committee and carried out in accordance with the guidelines of the Canadian Council of Animal Care.

Hemodynamics. Aortic root and left ventricular blood pressure measurements were performed in triplicate on a subset of mice (n = five) under isoflurane anesthesia using a Millar pressure-transducing catheter introduced through the right common carotid artery before they were killed, as described (29).

Tissue histology and immunohistochemistry. Kidneys were rapidly dissected, fixed overnight in 10% buffered formalin, and embedded in paraffin, and 4-μm sections underwent periodic acid-Schiff (PAS) staining. Glomerular volume and mesangial matrix area relative to total glomerular area were quantified in 20–30 glomeruli from each group by ImageJ software or Image Probe. The thickness of the glomerular basement membrane (GBM) was detected by electron microscopy (Department of Pathology, Mount Sinai Hospital, Toronto, Ontario, Canada). Images were captured by an Olympus ATM1600 camera system, and the thickness of the GBM was analyzed using the ruler function of the software (Olympus XL Docu). The average GBM thickness for each mouse was calculated from 95–225 measurements obtained from different GBM sites, from 9 images of 3 random glomeruli from each mouse.

Isolation of mouse glomeruli. Mouse glomeruli were isolated as previously described (30). Briefly, mice were anesthetized and perfused through the heart with 40 mL magnetic 4.5-μm diameter Dynabeads (Invitrogen) in PBS. Kidneys were minced into small pieces and digested with collagenase A (Roche) at 37°C for 30 min, filtered with a 100-μm cell strainer, and the glomeruli containing the Dynabeads were collected by a magnetic particle concentrator.

Immunohistochemistry. Collagen IV immunohistochemistry was performed on 4-μm sections that were deparaffinized, rehydrated, and blocked with 3% H_2O_2, followed by antigen retrieval in a microwave oven. Staining was done using 1:2,000 rabbit polyclonal collagen IV antibody and visualized using a Super Sensitive Polymer-HRP IHC Detection System/DAB kit (BioGenex) according to the manufacturer's instructions. Slides were digitized using a bright field scanner (ScanScope XT) and analyzed with Image-Pro software (Media Cybernetics). WT-1 staining was performed using WT-1 antibody (1:100; Santa Cruz Biotechnology). Color development was done with freshly prepared Nova Red solution (Vector Laboratories). Sections were counterstained lightly with Mayer's hematoxylin, dehydrated in alcohols, cleared in xylene, and mounted in Permount (Fisher Scientific) (31). The podocyte number was determined by counting the average number of positive-staining nuclei per glomerulus, from 40–50 glomeruli/mouse (n = five per group). All pathological analyses were performed blinded and verified by two observers.

Statistical analysis. The experimental data are reported as means ± SEM. Statistical differences among groups were assessed by ANOVA with a Tukey post hoc test for multiple comparisons. $P < 0.05$ was considered to be statistically significant.

RESULTS

High glucose induces Src-dependent EGFR transactivation through TACE. Treatment of mesangial cells with high glucose resulted in a time-dependent increase in Src Tyr-416 phosphorylation, a marker of Src activation (11,12), determined by immunoprecipitation, followed by immunoblotting with SrcpTyr-416 antibodies (Fig. 1*A*). This was not due to osmotic effects because mannitol had no effect (Supplementary Fig. 1*A*). Because Src has been reported to participate in EGFR transactivation, we examined EGFR tyrosine phosphorylation using site-specific antibodies. Phosphorylation of EGFR Tyr-845 was stimulated by high glucose, peaking at 48 h (Supplementary Fig. 1*B*). Two structurally distinct small molecule Src kinase inhibitors, PP2 (32) and SU6656 (33) used at low concentrations, 2 and 2.5 μmol/L, respectively, blocked high glucose–induced EGFR Tyr-845 phosphorylation (a Src kinase site) (Fig. 1*B*). As depicted in Fig. 1*C* and Supplementary Fig. 1*C*, high glucose also enhanced EGFR phosphorylation at Tyr-1173 (an EGFR autophosphorylation site), and this was also prevented by PP2. Because PP2 does not affect EGF-stimulated EGFR phosphorylation (34 and data not shown), these results indicate that EGFR kinase activity activated by high glucose required Src kinase. EGFRTyr-845 phosphorylation by Src appears to require ligand binding and activation (35). Consistent with this notion, AG1478, an

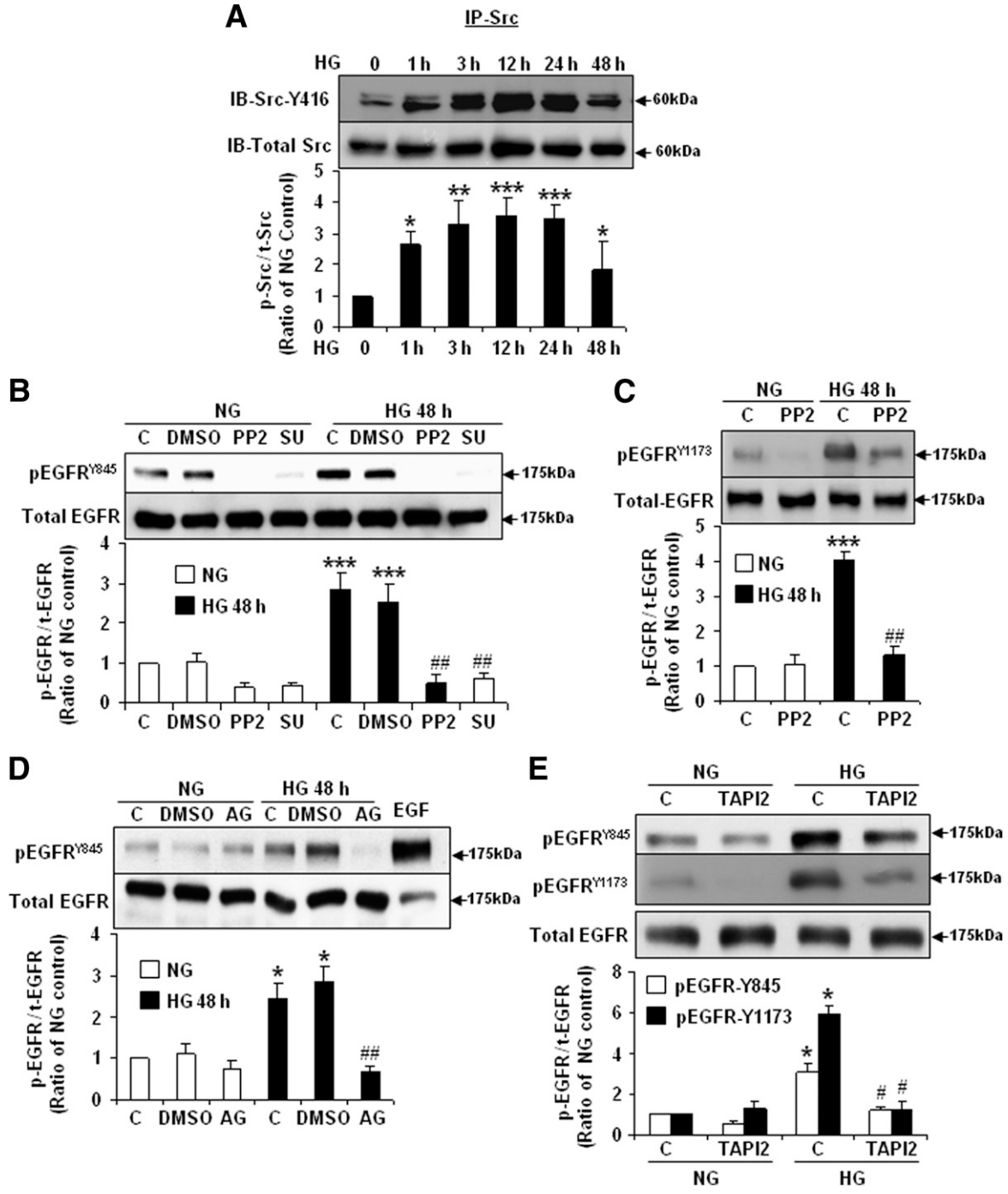

FIG. 1. High glucose (HG) causes Src-dependent EGFR transactivation via TACE. Mesangial cells (MC) were growth-arrested in 5.6 mmol/L normal glucose (NG) or 25 mmol/L HG for up to 48 h. *A*: Src was immunoprecipitated with anti-Src monoclonal antibodies from cell lysates, followed by immunoblotting with anti-pSrc$^{Tyr\text{-}416}$ antibodies (Src autophosphorylation site) and reprobed with anti-Src antibodies. *B*: EGFR Tyr-845 phosphorylation (Src phosphorylation site) and total EGFR levels in MC treated with or without the Src inhibitors, 2 μmol/L PP2 or 2.5 μmol/L SU6656 (SU), for the final 24 h. *C*: EGFR Tyr-1173 phosphorylation (autophosphorylation site) and total EGFR levels in cells treated with or without 2 μmol/L PP2 for 24 h. *D*: EGFR Tyr-845 phosphorylation (Src phosphorylation site) and total EGFR levels in cells treated with the EGFR kinase inhibitor, 200 nmol/L AG1478 (AG), for 48 h. *E*: EGFR pTyr-845 and pTyr-1173 and total EGFR immunoblots in cells grown in the presence or absence of 100 μmol/L TAPI-2 for 48 h. Results from four to six independent experiments are quantified in the graphs. C, control. *$P < 0.05$, **$P < 0.01$, ***$P < 0.001$ vs. NG; #$P < 0.05$, ##$P < 0.001$ vs. HG DMSO control.

EGFR kinase inhibitor, blunted EGFR Tyr-845 phosphorylation stimulated by high glucose (Fig. 1*D*). Together, these results suggested that high glucose induced mesangial cell EGFR transactivation through Src kinase stimulation.

Ectodomain shedding of transmembrane EGFR ligands can be evoked by ADAMs (23–27). To investigate the transactivation of EGFR by high glucose, we focused on ADAM-17/TACE because it has been documented to mediate EGFR transactivation by serotonin (25). The hydroxamic acid–based TACE inhibitor, TAPI-2 (36,37), diminished the stimulatory effect of high glucose on EGFR Tyr-845 and Tyr-1173 phosphorylation (Fig. 1*E*). These results suggest

that TACE plays a functional role in EGFR transactivation in this context.

TACE is activated by high glucose and is dependent on Src. To confirm the role of TACE and determine the requirement of Src, TACE activity and its membrane translocation were assessed. A TACE assay that used a fluorogenic substrate peptide with a TACE cleavage site revealed that high glucose stimulated a fourfold increase of activity, which was blocked by the Src inhibitors PP2 and SU6656 (Fig. 2*A*). To determine the specific role of Src kinase in high glucose using a genetic approach, mesangial cells were transfected with Src-specific siRNAs (siRNA1, siRNA2) or with a negative universal control siRNA to suppress the expression of endogenous Src. Transfection of siRNA2 decreased Src protein content by 77% (0.33 ± 0.08 compared with scrambled siRNA) and did not alter the SFKs, Fyn, or Yes (Supplementary Fig. 2*A* and *B*), and so was used in subsequent experiments. Src siRNA2 inhibited TACE activation in high glucose (Fig. 2*B*). In addition, immunoblotting (Fig. 2*C* and *D*) and confocal immunofluorescence microscopy (Fig. 2*E* and *F*) demonstrated increased TACE protein content in cell membrane fractions and TACE translocation from cytosol to the cell membrane in response to high glucose. The plasma membrane compartments were confirmed by immunoblotting of cell fractions for the plasma membrane marker, Na^+/K^+ ATPase α1 (Supplementary Fig.2*C*), and by loading cells with the plasma membrane dye, FM 4–64 Fx, for immunofluorescence (Supplementary Fig. 3). These effects on TACE were attenuated by chemical inhibition of Src kinase (PP2 and SU) and by knockdown with Src-siRNA (Fig. 2). These data, together with the inhibition of EGFR transactivation by blocking TACE, indicate that Src plays a key role in TACE-mediated ectodomain shedding of EGFR ligand in mesangial cells, leading to EGFR transactivation by high glucose.

High glucose–stimulated ERK phosphorylation requires Src, TACE, and EGFR. MAPKs, such as ERK1/2 (ERK) and p38 MAPK, are high glucose effectors that mediate mesangial cell ECM protein synthesis (8). High glucose stimulated a dose-dependent increase in ERK1/2 and p38 phosphorylation (Supplementary Fig 1*D*). Pretreatment of mesangial cells with either of the Src inhibitors, PP2 or SU6656 (Fig. 3*A*), eliminated ERK phosphorylation in the presence of high glucose. In accordance with ERK and p38 being downstream of EGFR in the setting of high glucose, antagonists of EGFR kinase, AG1478 and TACE (TAP1-2), all attenuated ERK and p38 phosphorylation elicited by high glucose (Fig. 3*B* and *C*).

Src is the SFK member activated by high glucose and required for EGFR and MAPK phosphorylation. Of several members of the family of SFKs (11,12), three ubiquitous members, Src, Yes, and Fyn, were expressed in the cultured mesangial cells (Supplementary Fig. 4). Immunoprecipitation with specific antibodies and immunoblotting with anti-Src pY-416 (which cross-reacts with the pY activation sites of other SFKs) revealed a transient activation by high glucose of Fyn (which reached maximum at 3–12 h) and no effect on Yes (Supplementary Fig. 4*A*–*D*). However, Fyn-specific siRNA, which had no effect on Src protein expression (Supplementary Fig. 5*A*), did not block high glucose–induced phosphorylation of EGFR Tyr-1173 or Tyr-845 (Supplementary Fig. 5*B*) or high glucose–stimulated p38 or ERK1/2 phosphorylation (Supplementary Fig. 5*C* and *D*). Consistent with the proposed specificity of Src to activate TACE and release EGFR ligand, the transfection of Src-specific siRNA2 resulted in a significant reduction of EGFR (Fig. 4*A*) and MAPK (p38 and ERK) (Fig. 4*B*) phosphorylation in high glucose. Together, these data indicate that in mesangial cells, Src is the major SFK responsible for signaling to MAPK in high glucose.

High glucose stimulation of collagen IV accumulation is mediated by a Src-TACE-EGFR-MAPK–signaling pathway. Excessive glomerular collagen IV deposition consequent to hyperglycemia is one of the key events in the development of diabetic glomerulosclerosis (1–6). To evaluate collagen IV levels, mesangial cells underwent immunofluorescence staining for collagen IV detected by confocal microscopy and immunoblotting of cell lysates. Collagen IV protein expression was increased by high glucose (Fig. 5). This effect was blocked in cells treated with the Src inhibitor, PP2 (Fig. 5*A* and *B*), and in cells transfected with Src-specific siRNA (Fig. 5*C* and *D*). Inhibition of EGFR with AG1478 or TACE with TAPI-2 also prevented high glucose–stimulated collagen IV expression (Fig. 5*A*). Thus, analogous to the GPCR-triggered TMS pathway (36–38), high glucose engages MAPKs and stimulates collagen IV synthesis through Src, TACE, and EGFR.

Inhibition of Src kinase activity blocks the Src-TACE-EGFR-MAPK–signaling pathway in the kidney in a murine model of type 1 diabetes. To address the in vivo role of Src, DBA2/J mice, reported to be particularly susceptible to diabetic nephropathy (28,39), were treated with five low-dose injections of STZ as indicated by the Animal Models of Diabetes Complications Consortium protocol (28). PP2 was administered beginning 3 weeks after the STZ injections. Six-hour fasting blood glucose levels 3 weeks after STZ administration were elevated (range 15–33 mmol/L) compared with vehicle-injected control mice (range 8.4–9.8 mmol/L) and were not altered by PP2 administration (Supplementary Table 1*A*). Glucose levels remained similarly elevated in diabetic mice until they were killed (not shown). Untreated control (nondiabetic) and PP2-treated nondiabetic mice demonstrated similar weight gain, as expected. However, neither untreated nor PP2-treated diabetic groups gained weight after STZ administration (Supplementary Table 1*B*). Kidney weight-to-body weight ratio was significantly increased only in the untreated diabetic mice (Supplementary Table 1*C*). To exclude effects of PP2 on blood pressure, aortic and left ventricular pressures were measured as described (29) after 6 weeks of diabetes. No significant differences were observed between PP2 treated and untreated groups (Supplementary Table 1*D*). The tendency to a lower blood pressure in both diabetic groups was likely due to a hyperglycemia-induced modest degree of fluid loss.

To determine the role of Src in vivo, renal cortical extracts were immunoblotted after 18–24 weeks of diabetes and showed an increase in Src Tyr-416 phosphorylation in total lysates (Fig. 6*A*) as well as after immunoprecipitation with Src-specific antibodies (Supplementary Fig. 6*A*), but there was no change in total or Tyr phosphorylated Fyn (Supplementary Fig. 6*B* and *C*). The Src Y-416 phosphorylation was abrogated by the Src inhibitor, PP2, for up to 24 h after administration, confirming its vivo efficacy (Fig. 6*A*). We also observed enhanced EGFR (Tyr-845 and Tyr-1173) phosphorylation in renal cortical membrane fractions from the diabetic mice, which was abolished by PP2 treatment (Figs. 6*B* and 7*C*). Furthermore, PP2 diminished the increase in phosphorylation of MAPKs (ERK1/2 and p38) in the renal cortex (Figs. 6*D* and 7*E*). Because the renal cortex contains tubules as well as glomeruli, and Src,

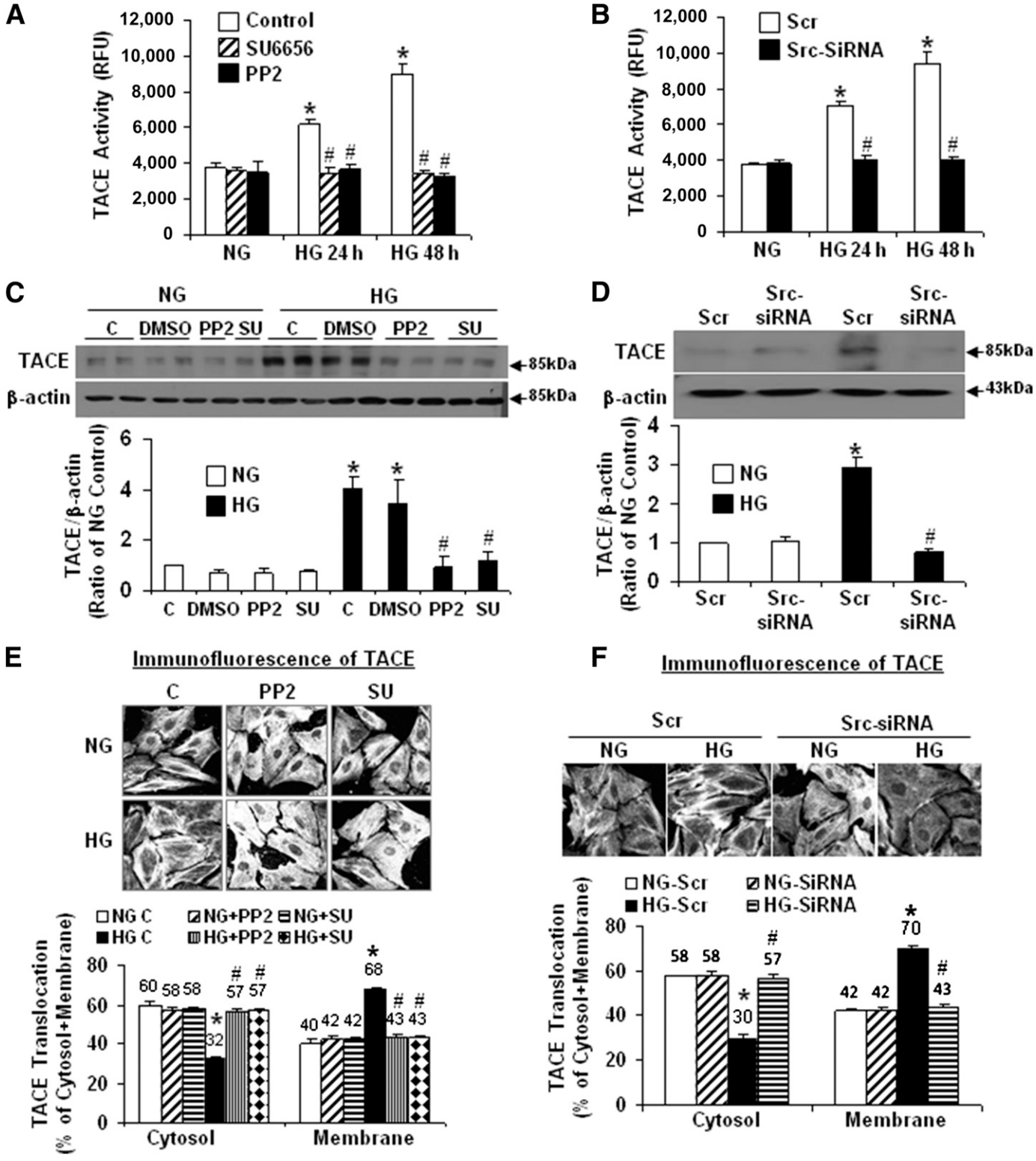

FIG. 2. High glucose (HG) induces Src-dependent TACE translocation and activation. Mesangial cells were incubated in 5.6 mmol/L normal glucose (NG) or 25 mmol/L HG for 48 h with and without 2 μmol/L PP2 or 2.5 μmol/L SU6656 for 24 h (*A*), or were transfected with Src-specific siRNA2 (5 nmol/L) or with scrambled control siRNA (Scr) (*B*). *A* and *B*: In vitro proteolytic activity of TACE was measured by cleavage of a fluorogenic substrate (RFU, relative fluorescence units) from four to eight independent experiments. *C* and *D*: TACE immunoblots of membrane fractions. Results from three to seven independent experiments are quantified in the graphs below the figures. The membrane marker Na^+/K^+ ATPaseα-1 was immunoblotted to verify purity (Supplementary Fig. 2*C*). *E* and *F*: Membrane translocation of TACE in response to HG was detected by immunofluorescence confocal imaging. The graphs represent the percentage of TACE protein distributed in plasma membrane (PM) and cytosolic compartments (see Supplementary Fig. 3 for outline of PM using the fluorescent dye, FM 4-64Fx). TACE immunofluorescence was quantified as pixel intensity of each of the compartments (the PM was considered as the area within a 3-mm distance from the cell surface). Values ± SE (n = 95–158 cells) in three separate experiments are shown below the immunofluorescence images. C, control. *$P < 0.001$ vs. NG-C or NG-Scr; #$P < 0.001$ vs. HG-C or HG-Scr.

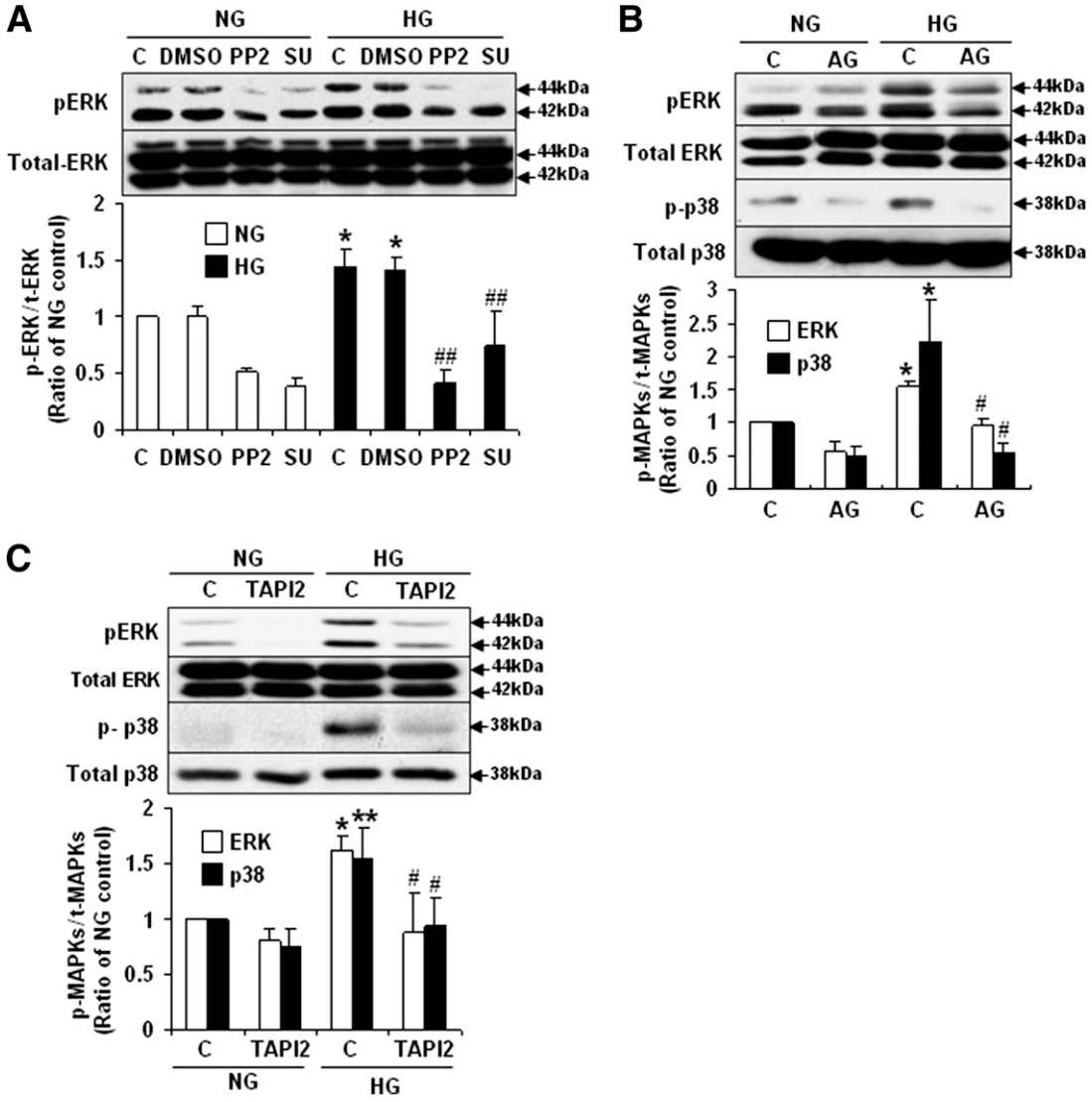

FIG. 3. High glucose (HG)-induced ERK1/2 and p38 phosphorylation requires Src, EGFR, and TACE. Mesangial cells were incubated in 5.6 mmol/L normal glucose (NG) or 25 mmol/L HG for 48 h. Phospho-(p)ERK1/2, phospho-p38, total ERK1/2, and total p38 levels were assessed by immunoblotting. Cells were treated with or without 2 μmol/L PP2 or 2.5 μmol/L SU6656 (SU) for 24 h (*A*), 200 nmol/L AG1478 (AG) for 48 h (*B*), or 100 μmol/L TAPI-2 for 48 h (*C*). Results from three to five independent experiments are quantified in the graphs. Intensities of phosphoproteins were corrected for total protein content in each experiment. Phospho- and total ERK data represent ERK1 and ERK2 combined. C, control. *$P < 0.05$, **$P < 0.01$ vs. NG; #$P < 0.05$, ##$P < 0.001$ vs. HG DMSO control.

EGFR, and MAPKs have been reported to be activated in renal tubular cells by angiotensin (40), glomeruli were isolated from these groups of mice, and phosphorylation was assessed by immunoblotting. Diabetes augmented and treatment with PP2 inhibited the phosphorylation of Src Tyr-416 (Supplementary Fig. 7*A*), EGFR Tyr-1173 (Supplementary Fig. 7*B*), and p38 and ERK1/2 (Supplementary Fig. 7*C* and *D*).

To confirm the role of TACE in vivo, TACE activity was measured in the kidney cortex homogenates. TACE activity was enhanced approximately twofold (Fig. 7*A*), and immunoblotting demonstrated increased TACE protein accumulation in the membrane fractions (Fig. 7*B*). These changes were attenuated by treatment with PP2. TACE is known to cleave HB-EGF to release ligand from the cell membrane. Immunoblotting of kidney cortex membranes with anti–full-length/mature HB-EGF revealed a marked decrease in the presence of diabetes, consistent with cleavage and loss of the mature fragment, which was blocked by PP2 administration (Fig. 7*C*). These data support the activation of a Src-TACE-HB–EGF-EGFR-ERK–signaling pathway in the diabetic kidney.

Inhibition of Src prevents albuminuria, glomerular ECM protein accumulation, and podocyte depletion in a murine model of type 1 diabetes. Urinary albumin excretion, measured as albumin-to-creatinine ratio, was significantly elevated in vehicle-treated diabetic mice and markedly reduced by administration of PP2 (Fig. 7*D*). Glomerular volume was increased by diabetes, and this was significantly attenuated by PP2 treatment (Supplementary Table 1*E*). Glomerular ECM protein was evaluated by quantitative analysis of PAS and collagen IV staining. As expected, PAS staining (quantified as mesangial matrix fraction) and collagen IV expression were elevated in the glomeruli of mice with STZ-induced diabetes and significantly diminished by PP2 treatment (Figs. 7*E* and 8*A* and *B* and Supplementary Fig. 8). To assess podocyte injury, the kidney sections were stained with WT-1, and

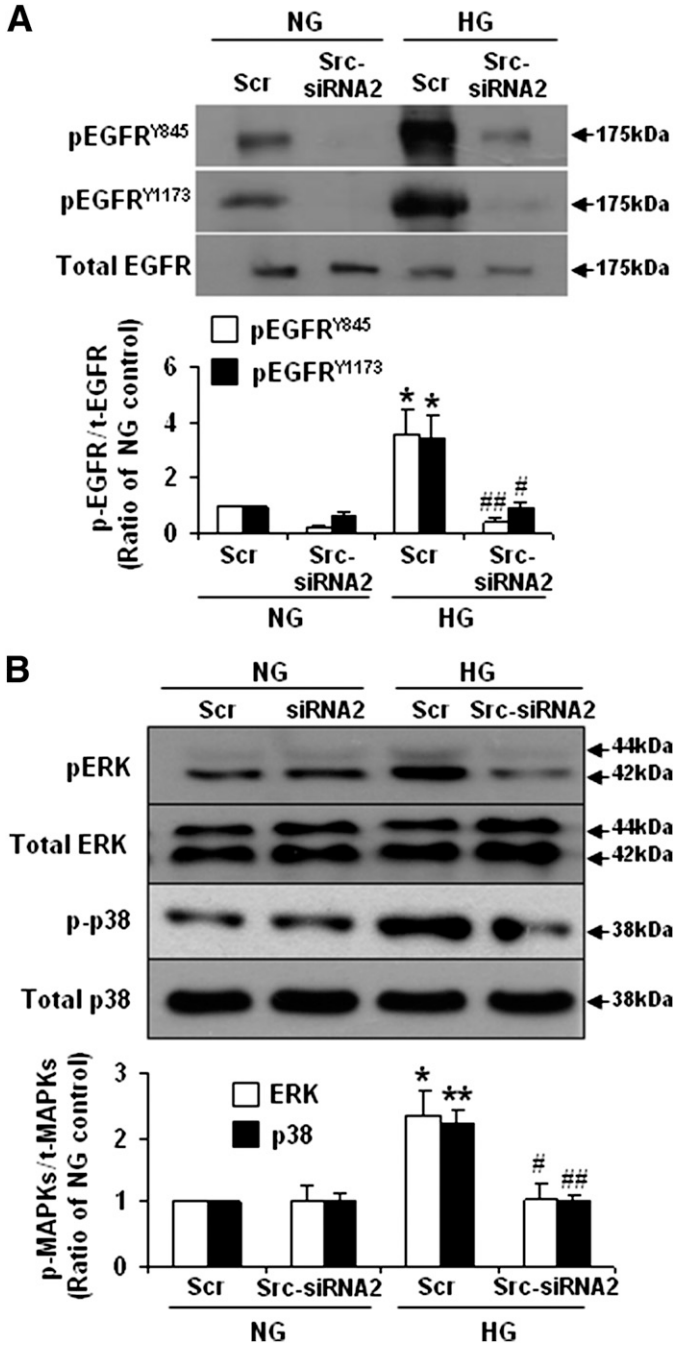

FIG. 4. Knockdown of Src inhibits high glucose (HG)-induced phosphorylation of EGFR and MAPKs. Mesangial cells were transfected with 5 nmol/L Src-specific siRNA2 or with scrambled control siRNA (Scr) in 5.6 mmol/L normal glucose (NG) for 24 h, then the cells were placed in NG or 25 mmol/L HG for 48 h. *A*: EGFR pTyr-845 and pTyr-1173 and total EGFR immunoblots. *B:* Phosphorylation of MAPK (p38, ERK). Graphs are representative of four independent experiments. *$P < 0.01$, **$P < 0.001$ vs. NG Scr; #$P < 0.05$, ##$P < 0.001$ vs HG Scr.

morphological changes were examined by electron microscopy as described in RESEARCH DESIGN AND METHODS. The number of podocytes determined by WT-1 staining was decreased by 28.5% in diabetic compared with nondiabetic mice. Treatment with PP2 preserved podocyte number in the diabetic mice (Fig. 8*C*). In addition, podocyte foot process effacement, along with increased GBM thickness, was found in diabetic mice, and PP2 administration inhibited these changes (Fig. 8*D*). These data demonstrate that in vivo Src inhibition can block or significantly reduce the manifestations of experimental diabetic nephropathy.

DISCUSSION

Current interventions for diabetic nephropathy, namely, control of blood glucose and hypertension and blockade of the renin-angiotensin system, are able to hinder but not stop the progressive loss of renal function that frequently accompanies diabetic nephropathy (41). Accordingly, new disease mediators and treatments continue to be sought. In this study, we explored the role of Src, an integrator of signaling pathways relevant to diabetic nephropathy. High glucose increased Src Tyr-416 phosphorylation in cultured mesangial cells as well as in the kidney cortex and glomeruli of mice with type 1 diabetes. Although we found evidence for transient activation of Fyn by high glucose in cultured mesangial cells, there was no evidence of long-term activation of this SFK member in the kidney of the diabetic mice. The functional consequences of Src-specific activation were demonstrated by chemical inhibitors as well as by siRNA-mediated Src knockdown. Thus, activation of TACE, EGFR, MAPK (ERK1/2 and p38), and collagen IV accumulation were all inhibited. Significantly, we showed that high glucose mimicked the TMS pathway, transactivating the EGFR via Src and TACE. High glucose–induced EGFR transactivation was manifested by EGFR Tyr-1173 and Tyr-845 phosphorylation. It should be noted that although EGFR activation may also stimulate Src, these data place Src upstream of EGFR signaling in the context of high glucose. The inhibition of phosphorylation of EGFRY845, a Src phosphorylation site, by the EGFR inhibitor, AG1478, is consistent with a ligand binding–dependent conformational change and activation of EGFR for this phosphorylation to take place (35). Transactivation by high glucose in cultured mesangial cells (10) and endothelin-dependent EGFR transactivation in the renal cortices of rats with type 2 diabetes (42) have been observed. Here, we demonstrated the involvement of Src in EGFR transactivation by high glucose using two distinct chemical inhibitors, PP2 and SU6656, as well as Src-siRNA. The further activation of EGFR, with maximum activation at 48 h (Supplementary Fig. 1) compared with maximum activation of Src at 12 h (Fig. 1), suggests that other downstream effectors of EGFR are also stimulated by high glucose.

TACE is the probable metalloproteinase releasing EGFR ligand in high glucose–treated mesangial cells based on the inhibition by TAPI-2 and the ability of high glucose in vitro and hyperglycemia in vivo to stimulate TACE activity and membrane translocation. In support of this concept, a number of studies have shown that TACE is involved in EGFR transactivation (37,38,43,44), and TACE/ADAM17 was the main sheddase for HB-EGF in a study of embryonic stem cells lacking various ADAMs (26). In mesangial cells, ADAM17, but not other ADAMs, immunoprecipitated with HB-EGF (25). Proteolytic release of a number of different cell surface–tethered EGFR ligands, such as TGF-α, HB-EGF, and amphiregulin, has been described to transactivate EGFRs (27,28,36). Our data in vivo, demonstrating the release of HB-EGF from kidney membranes of diabetic mice, are consistent with HB-EGF cleavage in high glucose. While this study was underway, Uttarwar et al. (10) reported in rat mesangial cells that ADAM17 (TACE) cleaves pro–HB-EGF, leading to high glucose–induced activation of the EGFR.

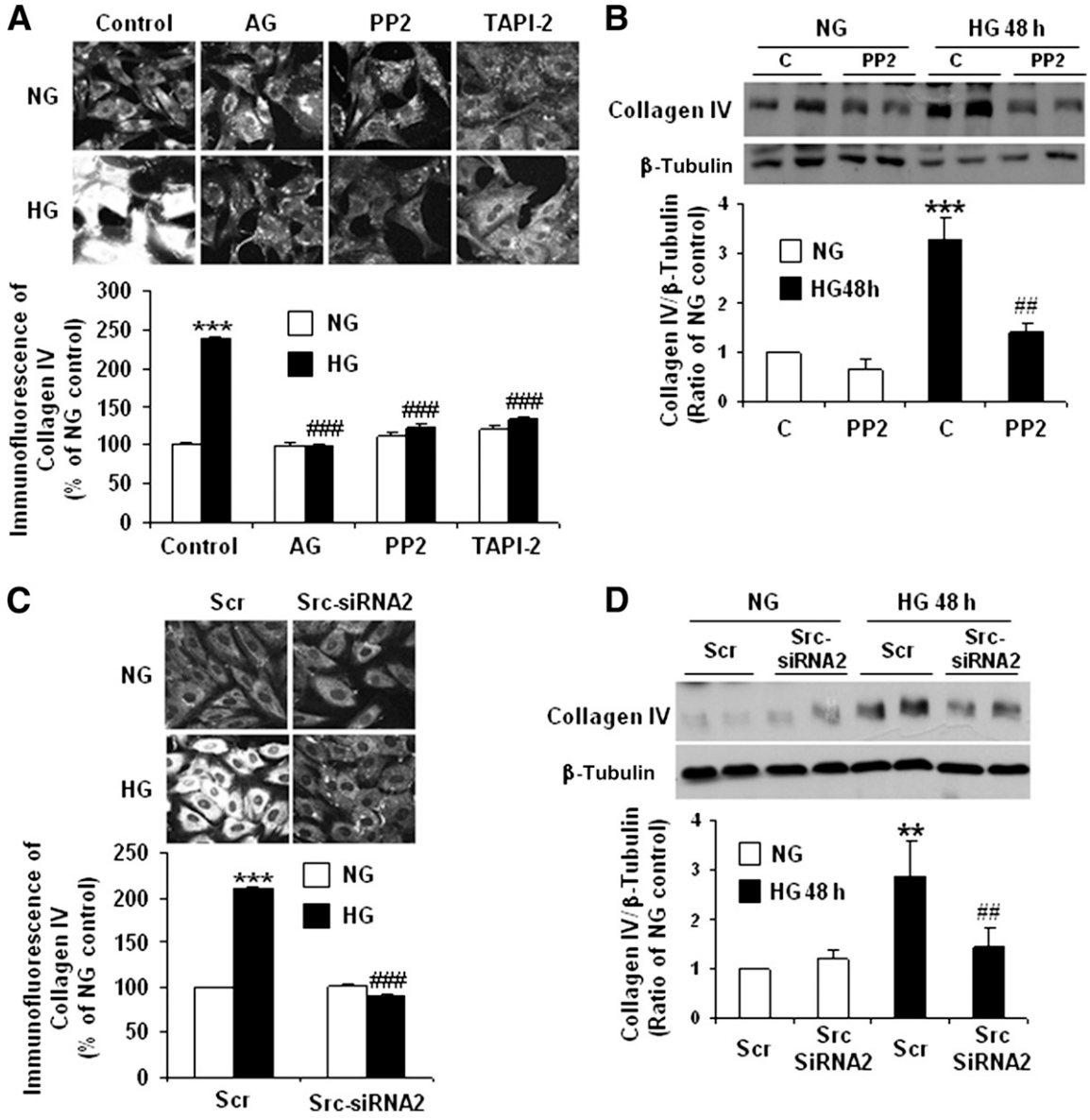

FIG. 5. High glucose (HG) stimulates collagen IV synthesis via EGFR, Src, and TACE. *A* and *B*: Mesangial cells were incubated in 5.6 mmol/L normal glucose (NG) or 25 mmol/L HG for 48 h and treated with or without 200 nmol/L AG1478 (AG), 2 μmol/L PP2, or 100 μmol/L TAPI-2. *C* and *D*: Mesangial cells were transfected with 5 nmol/L Src-specific siRNA2 or scrambled control siRNA (Scr), then exposed to 5.6 mmol/L NG or 25 mmol/L HG for 48 h. Collagen IV expression was analyzed by confocal immunofluorescence imaging (*A* and *C*) or immunoblotting (*B* and *D*). The graphs represent collagen IV immunofluorescence quantified as pixel intensity per cell (n = 87–201 cells) in 3 separate experiments or immunoblotting (mean ± SE) (n = 4–6). C, control. **P < 0.01 vs. NG control or NG-Scr; ***P < 0.001 vs. NG control or NG-Scr; ##P < 0.001 vs. HG or HG-Scr; ###P < 0.001 vs. HG or HG-Scr.

It has been proposed that TACE activity is upregulated by Ser/Thr phosphorylation of its cytoplasmic domain (43,45,46) by phosphoinositide-dependent kinase 1 (43) or ERK (47). However, in the current study, ERK was activated downstream rather than upstream of EGFR. As a reported target of TGF-β receptors, TACE activation was associated with translocation to the plasma membrane (48), similar to our findings in high glucose. Increased TACE expression, observed in angiotensin-infused mice (44), may also contribute to increased TACE activity. High glucose was also reported to stimulate TACE activity through PKC (27,45), but the role of Src in these studies was not examined. Although previous studies showed that HB-EGF transactivates EGFR in mesangial cells exposed to angiotensin, serotonin, or TGF-β (25,40,46,49), the current study is the first to demonstrate stimulation of TACE and HB-EGF ligand shedding in the diabetic kidney in vivo and its attenuation by inhibition of Src.

The upregulation of mesangial cell collagen IV mediated by Src and EGFR in the setting of high glucose is consistent with other observations. Thus, EGFR was linked to high glucose–induced synthesis of collagen I, which accumulates in late diabetic nephropathy (10). Src has also been implicated as a downstream mediator in TGF-β–stimulated collagen I and in angiotensin II–mediated type I and IV collagen and fibronectin synthesis in mesangial cells (13–15,18). In a recent study, the stimulation by angiotensin II was suggested to involve EGFR transactivation, and similar to our data, Src activation was implicated (40). However, in contrast to these findings in mesangial cells in high

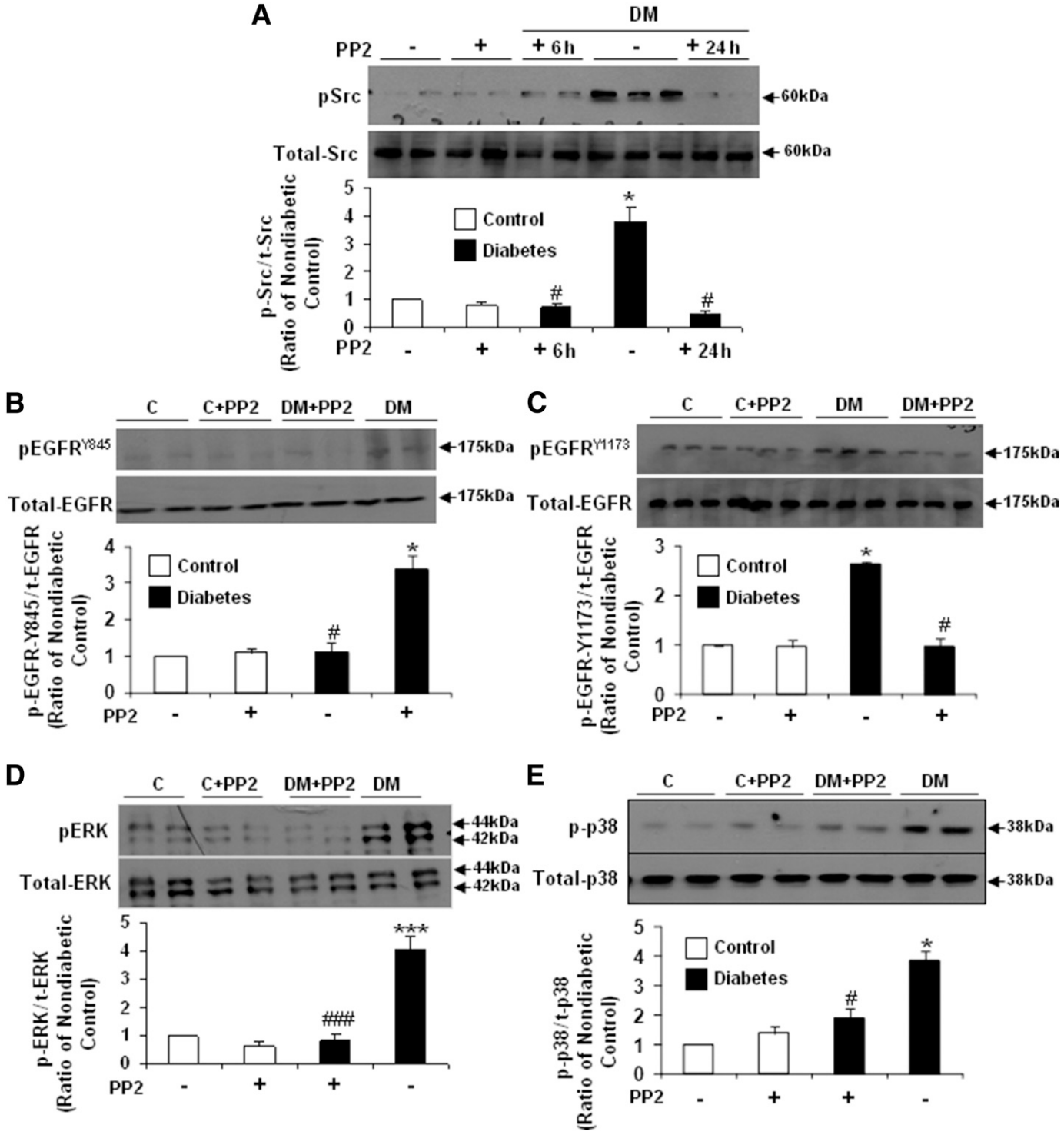

FIG. 6. PP2 administration inhibits phosphorylation of Src, EGFR, and MAPK in kidney cortex of STZ-induced diabetic mice. *A:* Src was immunoprecipitated from kidney cortex lysates and immunoblotted with anti-Src pTyr-416 and total Src. Mice were killed 6 or 24 h after their last PP2 injection. *B*: EGFR pTyr-845 and total EGFR levels. *C*: EGFR pTyr-1173 and total EGFR levels. *D* and *E*: Phospho-(p)ERK1/2, phospho-p38, and total ERK1/2, and total p38. Representative immunoblots of kidney cortex from separate mice. The graphs depict data (mean ± SE) from five to eight mice. C, control. *$P < 0.05$ vs. nondiabetic controls; #$P < 0.05$ vs. diabetic mice receiving vehicle alone; ***$P < 0.001$ vs. nondiabetic controls; ###$P < 0.001$ vs. diabetic mice receiving vehicle alone. DM, diabetic mice.

glucose, chronic EGFR activation in proximal tubular cells exposed to angiotensin was associated with Tyr-845 phosphorylation but not that of Tyr-1173, suggesting an alternate mechanism of activation (40).

We previously reported that the high glucose–induced increase in collagen IV in mesangial cells required NADPH oxidase (9). This ROS-generating pathway may interact with Src by stimulation of Src activity by NADPH oxidase (14) or, conversely, by an Src-mediated activation of NADPH oxidase (16). Further experiments will be required to define the role of NADPH oxidase and to identify whether Src is upstream and/or downstream of this enzyme in the setting

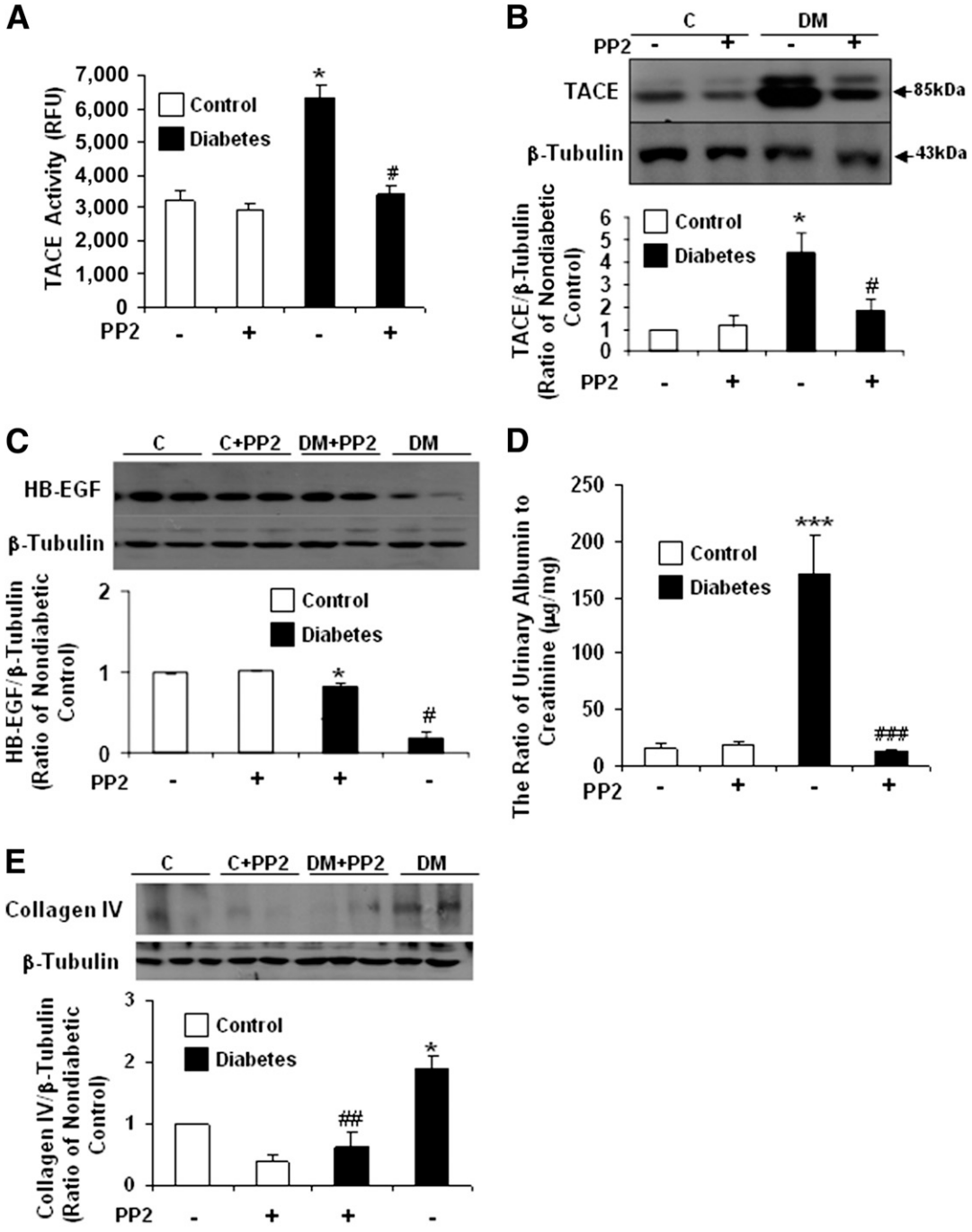

FIG. 7. PP2 administration decreases TACE activation, HB-EGF release, and collagen IV accumulation in kidney cortex and reduces albuminuria in STZ-induced diabetic mice. *A*: Proteolytic activity of TACE was measured by cleavage of a fluorogenic substrate from kidney cortex homogenates. RFU, relative fluorescence units. *B*: TACE immunoblots of kidney cortex membrane fractions. *C*: HB-EGF immunoblots of kidney cortex membrane fractions. *D*: Urinary albumin-to-creatinine ratio at 16 weeks in control and diabetic mice, treated or untreated with PP2. *E*: Collagen IV immunoblots of kidney cortex homogenates. Graphs represent values (mean ± SE) from five to seven mice. C, control. *$P < 0.05$ vs. nondiabetic controls; ***$P < 0.001$ vs. nondiabetic controls; #$P < 0.05$ vs. diabetic mice receiving vehicle alone; ##$P < 0.01$ vs. diabetic mice receiving vehicle alone; ###$P < 0.001$ vs. diabetic mice receiving vehicle alone. DM, diabetic mice.

of high glucose. In addition, Src could contribute to glomerular collagen IV accumulation by increasing PAI-1, an inhibitor of ECM protein degradation (7,50). Thus, although Src is a component of multiple signaling pathways that are activated in the kidney in the setting of diabetes (e.g., angiotensin II, TGF-β_1, platelet-derived growth factor, and vascular endothelial growth factor), it has not been implicated as a critical initiator or formally examined as a therapeutic target in diabetic nephropathy.

In STZ-induced diabetic mice, we detected elevated Src Tyr-416 phosphorylation in the kidney cortex and in isolated glomeruli, consistent with reports of increased glomerular Src phosphorylation in diabetic rats (17,18). However, in STZ-induced diabetic rats and mesangial cells exposed to angiotensin II, treatment with an angiotensin II receptor blocker, olmesartan, decreased glomerular Src Tyr-416 phosphorylation (18). In contrast, we observed that although angiotensin II stimulation of Src Tyr-416 phosphorylation

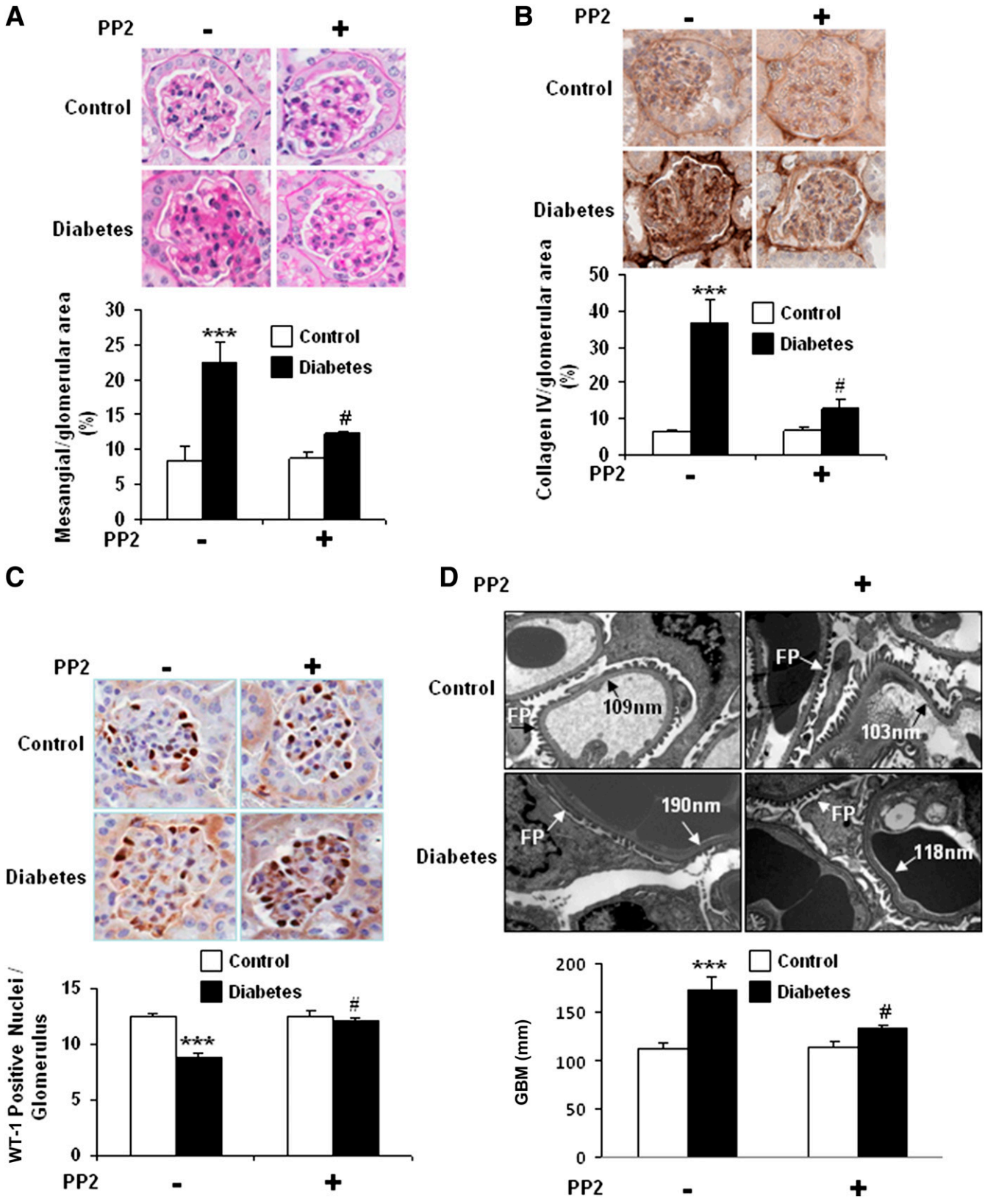

FIG. 8. PP2 reduces glomerular ECM proteins and collagen IV accumulation, podocyte depletion, GBM thickness, and podocyte foot process effacement in mice with STZ-induced diabetes. Diabetic and control mice were treated with or without PP2. *A*: PAS staining of glomeruli (n = 20–30 glomeruli per mouse). *B*: Collagen IV staining (immunohistochemistry) of glomeruli (n = 20–30 glomeruli per mouse). *C*: WT-I staining (immunohistochemistry) of glomeruli (n = 40–50 glomeruli per mouse). *D*: Glomerular foot process (FP) and GBM detected by electron microscopy. Arrows and values depict representative GBM in each group. Data were quantified and expressed as percent area (*A* and *B*), podocyte number (*C*), and the thickness of GBM (*D*) in the graphs below the representative figures, determined as described in RESEARCH DESIGN AND METHODS. Nondiabetic control, n = 7; nondiabetic mice treated with PP2, n = 5; untreated diabetic, n = 7; diabetic mice treated with PP2, n = 4. ***$P < 0$ 0.001 vs. nondiabetic control; #$P < 0.05$ vs. untreated diabetes.

in mesangial cells was blocked by losartan, stimulation by high glucose was not (Supplementary Fig. 9). This finding indicates that angiotensin II is not the sole mediator of high glucose signaling to Src. In the current study, we demonstrate for the first time that in vivo inhibition of Src prevents several manifestations of diabetic nephropathy, including albuminuria and glomerular pathologic changes (i.e., mesangial matrix protein and collagen IV accumulation and podocyte depletion). Podocyte loss in diabetic nephropathy has been associated with apoptosis (28). In contrast, Src activation has been found to promote cell survival and proliferation, particularly in the context of cancer (12,22,24,51). It should be noted that the data in this study do not implicate Src as a direct mediator of podocyte loss. Thus, whether Src is activated in podocytes by high glucose and its relationship to podocyte apoptosis in diabetic nephropathy requires further study. The above in vivo findings were accompanied by inhibition of the proposed signaling pathway, namely, a marked decrease in TACE activation and HB-EGF shedding along with EGFR and ERK phosphorylation in diabetic mice treated with PP2.

Although the specific role of Src in cell culture is supported by the siRNA knockdown experiments, the in vivo data with PP2 must be interpreted with caution because PP2 is not completely specific for Src and can inhibit several other kinases (52). Additional experiments with newer, more specific Src inhibitors as well as those compounds with different nonoverlapping kinase targets will be necessary to confirm that Src is a major target to prevent diabetic nephropathy in mice.

In summary, Src activation occurs in mesangial cells exposed to high glucose and in the kidneys of mice with STZ-induced type 1 diabetes. Activated Src mediates a high glucose–stimulated pathway leading to EGFR transactivation, MAPK activation, and collagen IV synthesis. In vivo treatment of type 1 diabetic mice with the Src inhibitor, PP2, prevented albuminuria, glomerular matrix protein accumulation, GBM thickening, and podocyte depletion, which correlate with progressive nephropathy. Thus, because Src may be activated by multiple pathways in the setting of high glucose, it may play a central role in pathogenesis and serve as an effective therapeutic target.

ACKNOWLEDGMENTS

This work was funded by grants from the Canadian Institutes of Health Research (CIHR) MOP 4l9409 and CCD 83025 (I.G.F.), the Canadian Diabetes Association (I.G.F.), and the Japan Diabetes Foundation and Uehara Memorial Foundation (K.T.), and in part by the University of Toronto Fred Sorkin Fund for Diabetes Research. E.A.Y.M. was supported in part by a postdoctoral fellowship from the Canadian Diabetes Association. K.W.K.L., A.S., and L.S. were supported in part by University of Toronto Banting and Best Diabetes Centre Novo Nordisk studentships.

No potential conflicts of interest relevant to this article were reported.

K.T. designed and conducted experiments and analyzed data. L.X. conducted experiments, analyzed data, and wrote the manuscript. H.J.G. analyzed data and wrote the manuscript. K.W.K.L. (in vitro), A.S., L.S., E.A.Y.M., A.M., E.A.S., and R.J. (in vivo) conducted experiments and analyzed data. M.H. contributed to discussion, analyzed data, and edited the manuscript. I.G.F. planned and supervised the study, designed experiments, analyzed data, and wrote the manuscript. I.G.F. is the guarantor of this work and, as such, had full access to all the data in the study and takes responsibility for the integrity of the data and the accuracy of the data analysis.

Parts of this study were presented in abstract form at the 72nd Scientific Sessions of the American Diabetes Association, Philadelphia, Pennsylvania, 8–12 June 2012.

The authors thank Albert Liang for technical help.

REFERENCES

1. Qian Y, Feldman E, Pennathur S, Kretzler M, Brosius FC 3rd. From fibrosis to sclerosis: mechanisms of glomerulosclerosis in diabetic nephropathy. Diabetes 2008;57:1439–1445
2. Fioretto P, Caramori ML, Mauer M. The kidney in diabetes: dynamic pathways of injury and repair. The Camillo Golgi Lecture 2007. Diabetologia 2008;51:1347–1355
3. Kanwar YS, Wada J, Sun L, et al. Diabetic nephropathy: mechanisms of renal disease progression. Exp Biol Med 2008;233:4–11
4. Mason RM, Wahab NA. Extracellular matrix metabolism in diabetic nephropathy. J Am Soc Nephrol 2003;14:1358–1373
5. Adler SG, Feld S, Striker L, et al. Glomerular type IV collagen in patients with diabetic nephropathy with and without additional glomerular disease. Kidney Int 2000;57:2084–2092
6. Matsubara T, Abe H, Arai H, et al. Expression of Smad1 is directly associated with mesangial matrix expansion in rat diabetic nephropathy. Lab Invest 2006;86:357–368
7. Huang Y, Border WA, Yu L, Zhang J, Lawrence DA, Noble NA. A PAI-1 mutant, PAI-1R, slows progression of diabetic nephropathy. J Am Soc Nephrol 2008;19:329–338
8. Haneda M, Koya D, Isono M, Kikkawa R. Overview of glucose signaling in mesangial cells in diabetic nephropathy. J Am Soc Nephrol 2003;14:1374–1382
9. Xia L, Wang H, Goldberg HJ, Munk S, Fantus IG, Whiteside CI. Mesangial cell NADPH oxidase upregulation in high glucose is protein kinase C dependent and required for collagen IV expression. Am J Physiol Renal Physiol 2006;290:F345–F356
10. Uttarwar L, Peng F, Wu D, et al. HB-EGF release mediates glucose-induced activation of the epidermal growth factor receptor in mesangial cells. Am J Physiol Renal Physiol 2011;300:F921–F931
11. Yeatman TJ. A renaissance for SRC. Nat Rev Cancer 2004;4:470–480
12. Bromann PA, Korkaya H, Courtneidge SA. The interplay between Src family kinases and receptor tyrosine kinases. Oncogene 2004;23:7957–7968
13. Mishra R, Zhu L, Eckert RL, Simonson MS. TGF-beta-regulated collagen type I accumulation: role of Src-based signals. Am J Physiol Cell Physiol 2007;292:C1361–C1369
14. Block K, Eid A, Griendling KK, Lee DY, Wittrant Y, Gorin Y. Nox4 NAD(P)H oxidase mediates Src-dependent tyrosine phosphorylation of PDK-1 in response to angiotensin II: role in mesangial cell hypertrophy and fibronectin expression. J Biol Chem 2008;283:24061–24076
15. Yano N, Suzuki D, Endoh M, Zhao TC, Padbury JF, Tseng YT. A novel phosphoinositide 3-kinase-dependent pathway for angiotensin II/AT-1 receptor-mediated induction of collagen synthesis in MES-13 mesangial cells. J Biol Chem 2007;282:18819–18830
16. Gianni D, Bohl B, Courtneidge SA, Bokoch GM. The involvement of the tyrosine kinase c-Src in the regulation of reactive oxygen species generation mediated by NADPH oxidase-1. Mol Biol Cell 2008;19:2984–2994
17. Suzaki Y, Yoshizumi M, Kagami S, et al. BMK1 is activated in glomeruli of diabetic rats and in mesangial cells by high glucose conditions. Kidney Int 2004;65:1749–1760
18. Mima A, Matsubara T, Arai H, et al. Angiotensin II-dependent Src and Smad1 signaling pathway is crucial for the development of diabetic nephropathy. Lab Invest 2006;86:927–939
19. Wieduwilt MJ, Moasser MM. The epidermal growth factor receptor family: biology driving targeted therapeutics. Cell Mol Life Sci 2008;65:1566–1584
20. Shah BH, Farshori MP, Jambusaria A, Catt KJ. Roles of Src and epidermal growth factor receptor transactivation in transient and sustained ERK1/2 responses to gonadotropin-releasing hormone receptor activation. J Biol Chem 2003;278:19118–19126
21. Van Schaeybroeck S, Kelly DM, Kyula J, et al. Src and ADAM-17-mediated shedding of transforming growth factor-alpha is a mechanism of acute resistance to TRAIL. Cancer Res 2008;68:8312–8321
22. Zhang Q, Thomas SM, Xi S, et al. SRC family kinases mediate epidermal growth factor receptor ligand cleavage, proliferation, and invasion of head and neck cancer cells. Cancer Res 2004;64:6166–6173

23. Prenzel N, Zwick E, Daub H, et al. EGF receptor transactivation by G-protein-coupled receptors requires metalloproteinase cleavage of proHB-EGF. Nature 1999;402:884–888
24. Schäfer B, Marg B, Gschwind A, Ullrich A. Distinct ADAM metalloproteinases regulate G protein-coupled receptor-induced cell proliferation and survival. J Biol Chem 2004;279:47929–47938
25. Göoz M, Göoz P, Luttrell LM, Raymond JR. 5-HT2A receptor induces ERK phosphorylation and proliferation through ADAM-17 tumor necrosis factor-alpha-converting enzyme (TACE) activation and heparin-bound epidermal growth factor-like growth factor (HB-EGF) shedding in mesangial cells. J Biol Chem 2006;281:21004–21012
26. Sahin U, Weskamp G, Kelly K, et al. Distinct roles for ADAM10 and ADAM17 in ectodomain shedding of six EGFR ligands. J Cell Biol 2004;164:769–779
27. Herrlich A, Klinman E, Fu J, Sadegh C, Lodish H. Ectodomain cleavage of the EGF ligands HB-EGF, neuregulin1-beta, and TGF-alpha is specifically triggered by different stimuli and involves different PKC isoenzymes. FASEB J 2008;22:4281–4295
28. Brosius FC 3rd, Alpers CE, Bottinger EP, et al.; Animal Models of Diabetic Complications Consortium. Mouse models of diabetic nephropathy. J Am Soc Nephrol 2009;20:2503–2512
29. Mungrue IN, Gros R, You X, et al. Cardiomyocyte overexpression of iNOS in mice results in peroxynitrite generation, heart block, and sudden death. J Clin Invest 2002;109:735–743
30. Takemoto M, Asker N, Gerhardt H, et al. A new method for large scale isolation of kidney glomeruli from mice. Am J Pathol 2002;161:799–805
31. Yang W, Wang J, Shi L, et al. Podocyte injury and overexpression of vascular endothelial growth factor and transforming growth factor-beta 1 in adriamycin-induced nephropathy in rats. Cytokine 2012;59:370–376
32. Hanke JH, Gardner JP, Dow RL, et al. Discovery of a novel, potent, and Src family-selective tyrosine kinase inhibitor. Study of Lck- and FynT-dependent T cell activation. J Biol Chem 1996;271:695–701
33. Blake RA, Broome MA, Liu X, et al. SU6656, a selective src family kinase inhibitor, used to probe growth factor signaling. Mol Cell Biol 2000;20:9018–9027
34. Alexander LD, Ding Y, Alagarsamy S, Cui XL, Douglas JG. Arachidonic acid induces ERK activation via Src SH2 domain association with the epidermal growth factor receptor. Kidney Int 2006;69:1823–1832
35. Biscardi JS, Maa MC, Tice DA, Cox ME, Leu TH, Parsons SJ. c-Src-mediated phosphorylation of the epidermal growth factor receptor on Tyr845 and Tyr1101 is associated with modulation of receptor function. J Biol Chem 1999;274:8335–8343
36. Pikul S, McDow Dunham KL, Almstead NG, et al. Discovery of potent, achiral matrix metalloproteinase inhibitors. J Med Chem 1998;41:3568–3571
37. Kenny PA, Bissell MJ. Targeting TACE-dependent EGFR ligand shedding in breast cancer. J Clin Invest 2007;117:337–345
38. Rodland KD, Bollinger N, Ippolito D, et al. Multiple mechanisms are responsible for transactivation of the epidermal growth factor receptor in mammary epithelial cells. J Biol Chem 2008;283:31477–31487
39. Breyer MD. Stacking the deck for drug discovery in diabetic nephropathy: in search of an animal model. J Am Soc Nephrol 2008;19:1623–1624
40. Chen JC, Chen JK, Nagai K, et al. EGFR signaling promotes TGFβ-dependent renal fibrosis. J Am Soc Nephrol 2012;23:215–224
41. Mauer M, Zinman B, Gardiner R, et al. Renal and retinal effects of enalapril and losartan in type 1 diabetes. N Engl J Med 2009;361:40–51
42. Portik-Dobos V, Harris AK, Song W, et al. Endothelin antagonism prevents early EGFR transactivation but not increased matrix metalloproteinase activity in diabetes. Am J Physiol Regul Integr Comp Physiol 2006;290:R435–R441
43. Zhang Q, Thomas SM, Lui VW, et al. Phosphorylation of TNF-alpha converting enzyme by gastrin-releasing peptide induces amphiregulin release and EGF receptor activation. Proc Natl Acad Sci U S A 2006;103:6901–6906
44. Lautrette A, Li S, Alili R, et al. Angiotensin II and EGF receptor cross-talk in chronic kidney diseases: a new therapeutic approach. Nat Med 2005;11:867–874
45. Reddy AB, Ramana KV, Srivastava S, Bhatnagar A, Srivastava SK. Aldose reductase regulates high glucose-induced ectodomain shedding of tumor necrosis factor (TNF)-alpha via PKC-delta and TNF-alpha converting enzyme in vascular smooth muscle cells. Endocrinology 2009;150:63–74
46. Uchiyama-Tanaka Y, Matsubara H, Mori Y, et al. Involvement of HB-EGF and EGF receptor transactivation in TGF-beta-mediated fibronectin expression in mesangial cells. Kidney Int 2002;62:799–808
47. Yin J, Yu FS. ERK1/2 mediate wounding- and G-protein-coupled receptor ligands-induced EGFR activation via regulating ADAM17 and HB-EGF shedding. Invest Ophthalmol Vis Sci 2009;50:132–139
48. Wang SE, Xiang B, Guix M, et al. Transforming growth factor beta engages TACE and ErbB3 to activate phosphatidylinositol-3 kinase/Akt in ErbB2-overexpressing breast cancer and desensitizes cells to trastuzumab. Mol Cell Biol 2008;28:5605–5620
49. Uchiyama-Tanaka Y, Matsubara H, Nozawa Y, et al. Angiotensin II signaling and HB-EGF shedding via metalloproteinase in glomerular mesangial cells. Kidney Int 2001;60:2153–2163
50. Samarakoon R, Higgins SP, Higgins CE, Higgins PJ. TGF-beta1-induced plasminogen activator inhibitor-1 expression in vascular smooth muscle cells requires pp60(c-src)/EGFR(Y845) and Rho/ROCK signaling. J Mol Cell Cardiol 2008;44:527–538
51. Amorino GP, Deeble PD, Parsons SJ. Neurotensin stimulates mitogenesis of prostate cancer cells through a novel c-Src/Stat5b pathway. Oncogene 2007;26:745–756
52. Brandvold KR, Steffey ME, Fox CC, Soellner MB. Development of a highly selective c-Src kinase inhibitor. ACS Chem Biol 2012;7:1393–1398